

## FOR PEER REVIEW - CONFIDENTIAL

**Cell-sized liposome doublets reveal active cortical tension build up**

Tracking no: 26-08-2014-RA-eLife-04511

Joël Lemière (Institut Curie), Matthias Bussonnier (Institut Curie), Timo Betz (Institut Curie), Cécile Sykes (Institut Curie), and Kevin Carvalho (Institut Curie)

**Abstract:**

Cells are able to generate contractile forces and modulate their shape to fulfill their specific functions. The cell cortex, a thin actin shell bound to the plasma membrane, mediates these essential behaviours. It is the substrate for myosin activity which contributes to cortical tension build up, together with actin dynamics. Here, we dissect the sole effect of myosin II on cortical tension increase with a non-invasive method. Cell-sized biomimetic liposomes are arranged in doublets and covered with a stabilized actin cortex anchored to the membrane. The addition of myosin II minifilaments to this doublet triggers a shape change unambiguously related to cortical-tension increase. Our assay paves the way for a quantification of cortical-tension changes triggered by various actin-associated proteins in a cell-sized system.

**Impact statement:** The action of actin and myosin in the cell cortex is mimicked and quantified using the rounding up of liposome doublets

**Competing interests:** No competing interests declared

**Author contributions:**

Joël Lemière: ; Conception and design; Acquisition of data; Analysis and interpretation of data; Drafting or revising the article; Contributed unpublished essential data or reagents Matthias Bussonnier: ; Analysis and interpretation of data; Drafting or revising the article; Contributed unpublished essential data or reagents Timo Betz: ; Contributed unpublished essential data or reagents Cécile Sykes: ; Analysis and interpretation of data; Drafting or revising the article Kevin Carvalho: ; Conception and design; Acquisition of data; Analysis and interpretation of data; Drafting or revising the article; Contributed unpublished essential data or reagents

**Funding:**

ANR: Joël Lemière, Cécile Sykes, Kevin Carvalho, 09BLAN0283; ANR: Joël Lemière, Cécile Sykes, Kevin Carvalho, 12BSV5001401; ANR: Matthias Bussonnier, Cécile Sykes, 11JSV50002; FRM: Joël Lemière, Cécile Sykes, Kevin Carvalho, DEQ20120323737; Joël Lemière, Matthias Bussonnier, PhD Student fellowship; Fondation ARC pour la recherche sur le cancer: Joël Lemière, Kevin Carvalho, PhD Student/ Postdoc fellowship The funders had no role in study design, data collection and interpretation, or the decision to submit the work for publication.

**Datasets:**

N/A

**Ethics:**

Human Subjects: No Animal Subjects: No

**Author Affiliation:**

Joël Lemière(UMR 168 Physico-chimie Curie, Institut Curie, France; UMR 168, CNRS, France) Matthias Bussonnier(UMR 168 Physico-chimie Curie, Institut Curie, France; UMR 168, CNRS, France) Timo Betz(UMR 168 Physico-chimie Curie, Institut Curie, France; UMR 168, CNRS, France) Cécile Sykes(UMR 168 Physico-chimie Curie, Institut Curie, France; UMR 168, CNRS, France) Kevin Carvalho(UMR 168 Physico-chimie Curie, Institut Curie, France; UMR 168, CNRS, France)

**Dual-use research:** No

**Permissions:** Have you reproduced or modified any part of an article that has been previously published or submitted to another journal? No

# Cell-sized liposome doublets reveal active cortical tension build up

2 Joël Lemière<sup>a,b,c,d</sup>, Matthias Bussonnier<sup>a,b,c,d</sup>, Timo Betz<sup>a,b,c</sup>, Cécile Sykes<sup>a,b,c</sup> & Kevin  
Carvalho<sup>a,b,c</sup>

4 <sup>a</sup> Institut Curie, Centre de Recherche, Paris, F-75248 France

5 <sup>b</sup> CNRS, UMR 168, Paris, F-75248 France

6 <sup>c</sup> Sorbonne Universités, UPMC Univ Paris 06, UMR 168, Paris, F-75005 France

7 <sup>d</sup> Univ Paris Diderot, Sorbonne Paris Cité, Paris, F-75205 France

8

## Abstract

10 Cells are able to generate contractile forces and modulate their shape to fulfill  
their specific functions. The cell cortex, a thin actin shell bound to the plasma

12 membrane, mediates these essential behaviours. It is the substrate for myosin  
activity which contributes to cortical tension build up, together with actin dynamics.

14 Here, we dissect the sole effect of myosin II on cortical tension increase with a non-  
invasive method. Cell-sized biomimetic liposomes are arranged in doublets and

16 covered with a stabilized actin cortex anchored to the membrane. The addition of  
myosin II minifilaments to this doublet triggers a shape change unambiguously

18 related to cortical-tension increase. Our assay paves the way for a quantification of  
cortical-tension changes triggered by various actin-associated proteins in a cell-sized

20 system.

22    **Introduction**

Cells are highly dynamic and need to change their shape in almost all cellular  
24 events spanning from division and motility to tissue remodeling. One of the major  
components involved in these processes is the contractile actin cytoskeleton  
26 arranged in a sub-micrometer thick network linked to the plasma membrane,  
containing myosin motors, and called the acto-myosin cortex [1]. It drives cell-shape  
28 changes as well as cell polarization [2] and governs tissue remodeling [3]–[6]. This  
cortex also insures tension in cells, called cortical tension [7]–[9], modulated by  
30 membrane-cytoskeleton attachment, actin network organisation and myosin motor  
activity. Micromanipulation of cells allows to measure the cortical tension, which was  
32 found to be between 50 and 4000 pN/ $\mu$ m depending on cell type, myosin activity and  
actin dynamics [7], [10]–[12]. Moreover, as shown for cell doublets, cell-cell  
34 adhesion is able to modulate cortical tension [13], a mechanism that is involved in  
cell sorting for tissue formation [14]. Recently, acto-myosin cortices have been  
36 reconstructed on supported lipid bilayers [15] and on cell-sized liposomes [16] where  
those reconstructions allowed to understand how crosslinking, attachment to the  
38 membrane, and actin-filament length influence contraction by myosin activity and  
actin polymerization [17].

40    In this study, we determine cortical-tension changes by the use of cell-sized  
doublet liposomes around which an acto-myosin cortex is reproduced *in vitro*.  
42 Variations in cortical tension are quantified by analysing doublet-shape change. This  
approach is reminiscent of cell-cell doublets used to uncover the role of cell adhesion  
44 in cortical-tension change [14]. Our assay allows isolating the role of myosin motors  
on cortical-tension build up, independently of actin dynamics and membrane tension.

## Results

48 **Formation of liposome doublets**

Liposomes are obtained by electroformation [18] from a mixture of egg-phosphatidylcholine (EPC) and biotin-PEG lipids (**See Methods**). We take the advantage of biotin PEG lipids to stick liposomes together by adding streptavidin to the liposome solution (**See Methods**). In these conditions, several doublets are formed within 15 minutes (**Fig. 1A**).

54 **Attachment of actin on doublet liposomes**

Phalloidin-stabilized fluorescent actin filaments, obtained in the presence of biotinylated actin monomers, stick to the membrane of the preformed doublets through a biotin-streptavidin-biotin link (**Fig. 1B**) and form a crosslinked homogeneous coat, as already characterized on liposomes [16]. Note that the interface between the two liposomes is free of actin filaments (**Fig. 1C - i**). To avoid the use of fluorescent lipids that may affect membrane mechanics [19], this interface is visualized by fluorescently labelling the inside buffer of only one of the liposomes with 0.9  $\mu$ M of sulforhodamin B (SRB) (**See Methods and Fig. 1C - i**).

### Effect of myosin injection

64 Myosin II motors, which assemble into bipolar filaments, are injected in the observation chamber by exchanging the external solution using an H-shaped flow 66 chamber where doublets are imaged (**Fig. 1C - ii**). Myosin II motors trigger a shape change of the doublets within minutes (**Fig. 1C - iii**) and the following geometrical 68 characteristics of the liposome doublets are modified: the distance between liposome

centers (d), the radii of the liposomes 1 and 2,  $R_1$  and  $R_2$ , respectively ( $R_1 > R_2$ ), the  
70 radius of curvature of the interface  $R_i$ , the volume of the doublet  $V$ , the angles  
between the interface and the liposome 1 or 2,  $\theta_1$  and  $\theta_2$ , respectively. We define the  
72 total contact angle  $\theta_{tot} = \theta_1 + \theta_2$  (**Fig. 1D**). These parameters are geometrically  
linked (**Fig. 1D**), and obtained by adjusting two spherical caps in contact, either in  
74 2D- (phase contrast and epifluorescence) images or 3D-(spinning disk) stacks (**See  
Methods**). We use the total contact angle  $\theta_{tot}$  as a reporter for shape change. We  
76 find that myosin addition produces an increase of  $\theta_{tot}$ . Indeed, on epifluorescence  
images and in the absence of myosin, we measure a total contact angle  $\theta_{tot}$  of  $(64 \pm$   
78  $16)^\circ$  ( $n=18$ , standard deviation) whereas in the presence of 200 nM myosin and  
before the actin cortex ruptures, we find a  $\theta_{tot}$  value of  $(86 \pm 21)^\circ$  ( $n=5$ , standard  
80 deviation). This difference is statistically significant ( $p=0.0186$ )

### Angles are related to tensions

82 Liposomes 1 and 2 have uniform tensions  $\tau_1$  and  $\tau_2$  respectively. Tension  
refers to the sole membrane tension in the absence of actin and myosin, and to  
84 cortical tension in their presence. The tension at the interface between liposome 1  
and 2 has two components: a membrane tension  $\tau_i$  and the adhesion energy per unit  
86 surface  $W$  which is due to biotin-streptavidin-biotin adhesion, and reads  $(\tau_i - W)$ . The  
Young's equation, which relates tensions and angles, can be applied to the contact  
88 line between the two doublet liposomes (**Fig1. D**). When projected on the tangent to  
the interface between liposomes, the Young's equation reads:

$$90 \quad \tau_i - W = \tau_1 \cos \theta_1 + \tau_2 \cos \theta_2 \quad (1)$$

When projected orthogonally to the contact surface tangent, one finds:

$$\tau_1 \sin \theta_1 = \tau_2 \sin \theta_2 \quad (2)$$

### Contact-angle dispersion

94 Dispersion in  $\theta_{tot}$ , in a population of doublets before myosin injection is  $\pm 16^\circ$ .  
 It reflects a difference in tension, which could be due either to the dispersion of  
 96 tension during liposome preparation, or to a difference in adhesion at the interface  
 between doublet liposomes, or to contribution of the actin shell in tension build up.  
 98 Contact angle increase upon myosin addition and this dispersion, have roughly the  
 same value, which prompted us to characterize many individual doublets as a  
 100 function of time.

### The sole presence of an actin shell does not modify the contact angle

102 We now investigate how the actin shell affects the contact angle, and thus the  
 tension, in the absence of myosin. We compare the shape of the same doublet in the  
 104 presence or in the absence of an actin shell by photo-damaging the actin filamentous  
 network (**Fig. 2A**) [20]. The total contact angle changes only by  $(3.4 \pm 2)^\circ$  ( $n = 7$ ),  
 106 (**Fig. 2B**) which is negligible compared to the change due to myosin activity (see  
 above).

### 108 3D observations

The plane of epifluorescence images is generally not parallel to the doublet  
 110 equatorial plane ( $R_1/R_2$  varies between 1.15 and 1.82), hence leading to an  
 underestimate of the angle  $\theta_{tot}$ . Therefore, 3D spinning disk image stacks are  
 112 recorded (**Fig. 3A**) for an accurate determination of  $\theta_{tot}$ ,  $V$  and  $d$  (see above for  
 definition), which are obtained by fitting spherical caps on 3D stacks (**Fig.3\_figure**  
 114 **supplement 1** and **Methods**). All initial values before myosin addition are labelled

$\theta_{tot}^I$ ,  $V^I$ ,  $d^I$  and  $\theta_{tot}(t)$ ,  $V(t)$ ,  $d(t)$  after addition of 50 to 100 nM myosin II at t=0. We

116 observe that  $\theta_{tot}(t)$  increases, whereas  $d(t)$  decreases when myosin filaments are

added (**Fig. 3B-D**). During these geometric changes, the volume remains constant

118 within 10%, consistent with experiments performed on cell doublets [14], [21] (**Fig.**

**3D**).

120 Visual inspection of our images reveals that the interface between liposome 1

and 2 only differs from a flat interface by a few pixels (**Fig.3\_figure supplement 2**).

122 The curvature  $1/R_i$  (**Fig. 1D**) is generally much smaller than  $1/R_1$  and  $1/R_2$ , which are

comparable. This observation leads to the assumption that  $\theta_1 = \theta_2 = \theta$  within our

124 resolution.

## Discussion

126 **Cortical tension is homogeneous for a single doublet**

The use of **equation (2)** with  $\theta_1(t) = \theta_2(t) = \theta_{tot}(t)/2 = \theta(t)$  leads to the equality of

128 tensions on both sides of the doublet, thus,  $\tau_1(t) = \tau_2(t) = \tau(t)$ . This result is

consistent with the fact that actin is distributed continuously all around the liposome

130 doublet. Thus, myosin II mini-filaments contract a continuous shell. Under these

conditions, **equation (1)** simplifies to:

132 
$$\tau_i - W = 2\tau(t) \cdot \cos \theta(t), \quad (3)$$

with the reasonable assumption that  $\tau_i - W$  is considered constant over time for a

134 given doublet although it may depend on the variability of initial adhesion in our

experiments. Therefore, we obtain the tension  $\tau(t)$ , which varies during acto-myosin

136 contraction, by:

$$\tau(t) = \frac{\text{cst}}{2 \cdot \cos \theta(t)}. \quad (4)$$

138 The tension relative to its initial value reads:

$$\frac{\tau(t)}{\tau^I} = \frac{\cos \theta^I}{\cos \theta(t)} \quad (5)$$

140 **Relative increase of cortical tension**

Interaction of myosin II filaments with a biomimetic actin cortex induces  
 142 tension build up. The cortical tension, normalized to its initial value  $\frac{\tau(t)}{\tau^I}$ , increases and reaches a maximal value  $\frac{\tau^{max}}{\tau^I}$  (**Fig. 3E**). Conditions of myosin concentration (50 to  
 144 200nM) allow to visualise doublet deformations before cortex breakage (peeling [16]).  
 Cortex breakage however leads to the recovery of the doublet initial shape, before  
 146 myosin injection (**see dashed blue line for d and θ Fig. 3**). The relative maximal change in tension is found to be  $\frac{\tau^{max}}{\tau^I} = 1.56 \pm 0.56$  (n=5) in spinning-disk imaging  
 148 and  $\frac{\tau^{max}}{\tau^I} = 1.25 \pm 0.15$  (n=5) in epifluorescence. This difference is in agreement with the fact that contact angle is underestimates in epifluorescence (see above).

150 **Cortical-tension increase in doublets and in cells**

In cells, cortical tension can be as low as 50 pN/ $\mu$ m in fibroblast progenitor  
 152 cells [10] and can go up to 4000 pN/ $\mu$ m for dictyostelium [11]. Surprisingly, when myosin activity is impaired – either by drugs or by genetic manipulation – cortical  
 154 tension only decreases about twofold [7], [10], [11], [22]. Our *in vitro* reconstruction is able to capture this feature in the change of cortical tension. Indeed, we observe an  
 156 increase in cortical tension by a factor 1.1 to 2.4 upon addition of myosin II minofilaments.

158    **Different contributions for cortical tension**

Cortical tension is the sum of the membrane tension and the tension due to  
160 the actomyosin cortex. On average, in our assay, we find an increase of cortical  
tension of 1.56 relative to the situation with actin only. Cortical tension is unchanged  
162 by the presence of the sole actin shell (see above), therefore, membrane tension  
contributes for 64% to cortical tension in the presence of myosin. In suspended  
164 fibroblast cells however, membrane tension is estimated to be only 10% of the  
cortical tension [7]. This difference may be explained by the absence of actin  
166 dynamics in our assay, in line with the increase of cortical tension when  
polymerization is stimulated in cells [7], [13]. How actin polymerization contributes to  
168 cortical tension is still an open question that needs to be addressed taking into  
account the geometry of the cell with actin polymerization at the inner membrane  
170 leaflet. Whereas actin polymerization outside a liposome has been clearly shown to  
generate inward pressure, is not yet clear how this can be translated into tension in a  
172 different geometry. *In vitro* assays are on their way to mimic actin dynamics in cells  
[23], [24] and will allow unveiling the mechanism of tension build up by actin  
174 dynamics. This is the remaining module that needs to be understood, while the effect  
of myosin is distinguished from the one of membrane in this study.

176    **Conclusion**

We provide a biomimetic reconstitution of tension build up through acto-  
178 myosin contractility using liposome doublets. Cortical tension is monitored *in situ* over  
time by analysing changes in doublet shape. This method allows us to directly  
180 quantify the relative increase in tension due to myosin, separately from the one due  
to actin dynamics. Understanding contraction of composite systems built brick by

182 brick on the model of a cell tile the road for the reconstitution of complex systems like  
tissues.

184 Acknowledgments: This work was supported by the French Agence Nationale pour la  
Recherche (ANR), grant ANR 09BLAN0283, ANR 12BSV5001401 and ANR-11-  
186 JSV5-0002, and by the Fondation pour la Recherche Médicale (FRM), grant  
DEQ20120323737. We thank Dr Agnieszka Kawska at IlluScientia for schemes. JL  
188 and MB thank the AXA Research Fund for doctoral fellowships. JL and KC were also  
supported by la Fondation ARC pour la recherche sur le cancer. We thank Thomas  
190 Risler and Clément Campillo for critical reading of the manuscript

192 **Bibliography**

- [1] A. G. Clark, K. Dierkes, E. K. Paluch, « Monitoring Actin Cortex Thickness in  
194 Live Cells », *Biophys. J.*, vol. 105, n° 3, p. 570-580, 2013.
- [2] G. Salbreux, G. Charras, E. Paluch, « Actin cortex mechanics and cellular  
196 morphogenesis », *Trends Cell Biol.*, 2012.
- [3] E. Munro, J. Nance, J. R. Priess, « Cortical flows powered by asymmetrical  
198 contraction transport PAR proteins to establish and maintain anterior-posterior  
polarity in the early *C. elegans* embryo », *Dev. Cell*, vol. 7, n° 3, p. 413-424,  
200 2004.
- [4] T. Lecuit, P.-F. Lenne, « Cell surface mechanics and the control of cell shape,  
202 tissue patterns and morphogenesis », *Nat. Rev. Mol. Cell Biol.*, vol. 8, n° 8, p.  
633-644, 2007.
- [5] M. Rauzi, P.-F. Lenne, T. Lecuit, « Planar polarized actomyosin contractile flows  
204 control epithelial junction remodelling », *Nature*, vol. 468, n° 7327, p. 1110-1114,  
206 2010.
- [6] M. Rauzi P.-F. Lenne, « Cortical forces in cell shape changes and tissue  
208 morphogenesis », *Curr. Top. Dev. Biol.*, vol. 95, p. 93-144, 2011.

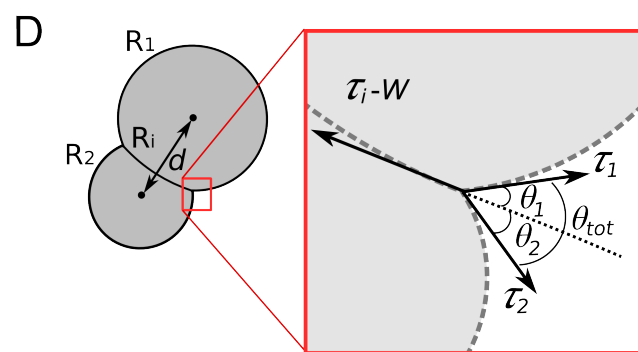
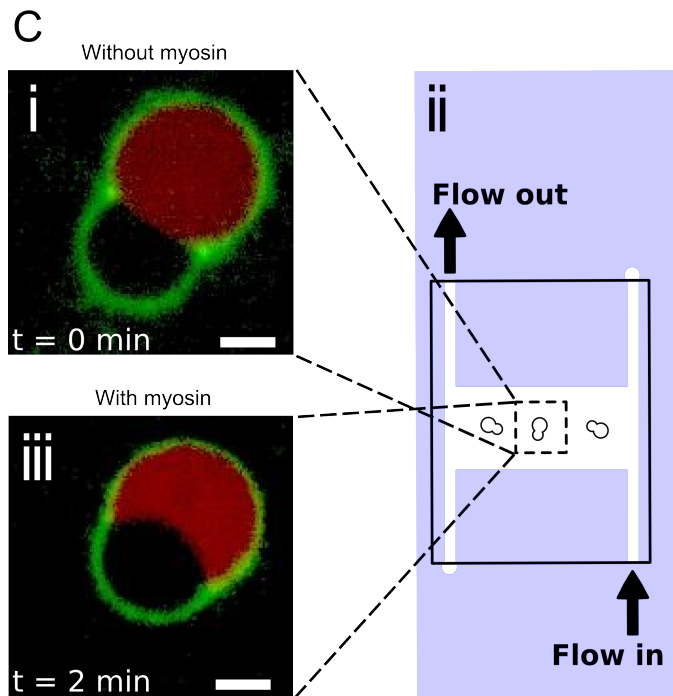
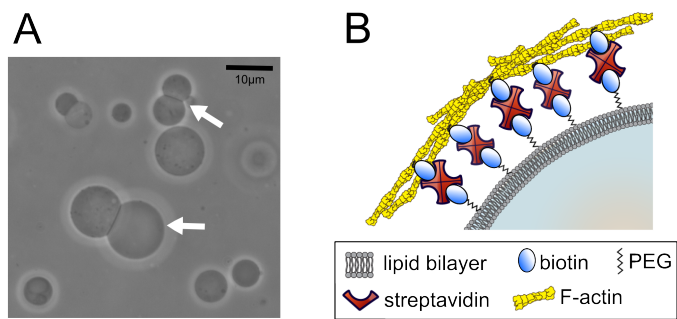
- [7] J.-Y. Tinevez, U. Schulze, G. Salbreux, J. Roensch, J.-F. Joanny, E. Paluch,  
210 « Role of cortical tension in bleb growth », *Proc. Natl. Acad. Sci. U. S. A.*, vol.  
106, n° 44, p. 18581-18586, 2009.
- [8] R. Nambiar, R. E. McConnell, M. J. Tyska, « Control of cell membrane tension  
by myosin-I », *Proc Natl Acad Sci U S A*, vol. 106, n° 29, p. 11972-11977, 2009.
- [9] D. Raucher, T. Stauffer, W. Chen, K. Shen, S. Guo, J. D. York, M. P. Sheetz, T.  
Meyer, « Phosphatidylinositol 4,5-bisphosphate functions as a second  
216 messenger that regulates cytoskeleton-plasma membrane adhesion », *Cell*, vol.  
100, n° 2, p. 221-228, 2000.
- [10] M. Krieg, Y. Arboleda-Estudillo, P.-H. Puech, J. Käfer, F. Graner, D. J. Müller,  
C.-P. Heisenberg, « Tensile forces govern germ-layer organization in  
220 zebrafish », *Nat. Cell Biol.*, vol. 10, n° 4, p. 429-436, 2008.
- [11] E. C. Schwarz, E. M. Neuhaus, C. Kistler, A. W. Henkel, T. Soldati,  
222 « Dictyostelium myosin IK is involved in the maintenance of cortical tension and  
affects motility and phagocytosis », *J. Cell Sci.*, vol. 113 ( Pt 4), p. 621-633,  
224 2000.
- [12] T. Luo, K. Mohan, P. A. Iglesias, D. N. Robinson, « Molecular mechanisms of  
226 cellular mechanosensing », *Nat. Mater.*, vol. 12, n° 11, p. 1064-1071, 2013.
- [13] W. Engl, B. Arasi, L. L. Yap, J-P. Thiery, V. Viasnoff, « Actin dynamics modulate  
228 mechanosensitive immobilization of E-cadherin at adherens junctions », *Nat. Cell Biol.*, vol. 16, n° 6, p. 587-594, 2014.
- [14] J.-L. Maître, H. Berthoumieux, S. F. G. Krens, G. Salbreux, F. Jülicher, E.  
Paluch, C.-P. Heisenberg, « Adhesion Functions in Cell Sorting by Mechanically  
232 Coupling the Cortices of Adhering Cells », *Science*, vol. 338, n° 6104, p. 253-  
256, 2012.
- [15] M. P. Murrell, M. L. Gardel, « F-actin buckling coordinates contractility and  
severing in a biomimetic actomyosin cortex », *Proc. Natl. Acad. Sci.*, 2012.
- [16] K. Carvalho, F. C. Tsai, E. Lees, R. Voituriez, G. H. Koenderink, C. Sykes,  
236 « Cell-sized liposomes reveal how actomyosin cortical tension drives shape  
change », *Proc. Natl. Acad. Sci.*, 2013.
- [17] K. Carvalho, J. Lemière, F. Faqir, J. Manzi, L. Blanchoin, J. Plastino, T. Betz, C.  
Sykes, « Actin polymerization or myosin contraction: two ways to build up  
cortical tension for symmetry breaking », *Philos. Trans. R. Soc. B Biol. Sci.*, vol.  
240 368, n° 1629, 2013.

- [18] M. Angelova, D. Dimitrov, « Liposome electroformation », *Faraday Discuss.*, vol. 81, p. 303+, 1986.
- [19] O. Sandre, L. Moreaux, F. Brochard-Wyart, « Dynamics of transient pores in stretched vesicles », *Proc. Natl. Acad. Sci. U. S. A.*, vol. 96, n° 19, p. 10591-10596, 1999.
- [20] J. van der Gucht, E. Paluch, J. Plastino, C. Sykes, « Stress release drives symmetry breaking for actin-based movement », *Proc. Natl. Acad. Sci. U. S. A.*, vol. 102, n° 22, p. 7847-7852, 2005.
- [21] J. Sedzinski, M. Biro, A. Oswald, J.-Y. Tinevez, G. Salbreux, E. Paluch, « Polar actomyosin contractility destabilizes the position of the cytokinetic furrow », *Nature*, vol. 476, n° 7361, p. 462-466, 2011.
- [22] P. Kunda, A. E. Pelling, T. Liu, B. Baum, « Moesin controls cortical rigidity, cell rounding, and spindle morphogenesis during mitosis », *Curr. Biol. CB*, vol. 18, n° 2, p. 91-101, 2008.
- [23] E. Abu Shah, K. Keren, « Symmetry breaking in reconstituted actin cortices », *eLife*, vol. 3, p. e01433, 2014.
- [24] T. Luo, V. Srivastava, Y. Ren, D. N. Robinson, « Mimicking the mechanical properties of the cell cortex by the self-assembly of an actin cortex in vesicles », *Appl. Phys. Lett.*, vol. 104, n° 15, p. 153701, 2014.
- [25] G. H. Koenderink, Z. Dogic, F. Nakamura, P. M. Bendix, F. C. MacKintosh, J. H. Hartwig, T. P. Stossel, D. A. Weitz, « An active biopolymer network controlled by molecular motors », *Proc. Natl. Acad. Sci. U. S. A.*, vol. 106, n° 36, p. 15192-15197, 2009.
- [26] Y. Y. Toyoshima, S. J. Kron, E. M. McNally, K. R. Niebling, C. Toyoshima, J. A. Spudich, « Myosin subfragment-1 is sufficient to move actin filaments in vitro », *Nature*, vol. 328, n° 6130, p. 536-539, 1987.
- [27] M. S. E. Silva, M. Depken, B. Stuhrmann, M. Korsten, F. C. Mackintosh, G. H. Koenderink, « Active multistage coarsening of actin networks driven by myosin motors », *Proc. Natl. Acad. Sci. U. S. A.*, 2011.

## Figure legends

274

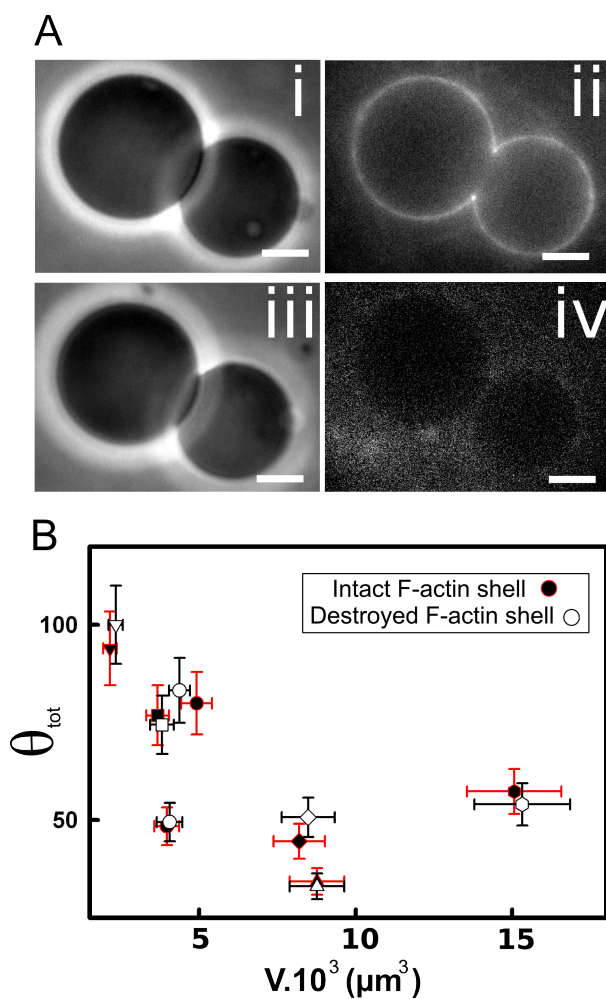
Figure 1: **Cell-sized liposome doublets.** A) Doublets, indicated by white arrows, in  
276 the field of view of a phase contrast microscope. B) Schematic of the stabilized actin  
cortex at the membrane (proteins not to scale). C) ii) Macrofluidics chamber designed  
278 to exchange the outside buffer. Doublets are visualized in the middle horizontal  
channel of the H shape chamber to avoid movement during the buffer exchange.  
280 Spinning disk images of the doublet before i) or after iii) myosin II injection. One  
liposome contains SRB (red) to visualize the interface of the doublet, the actin cortex  
282 is labelled in green. Scale bar 5 $\mu$ m. D) Scheme of the doublet with the three  
characteristic radii. Inset: enlargement of the contact interface between the two  
284 liposomes with the Young's tension vectors and the contact angles.



286

288

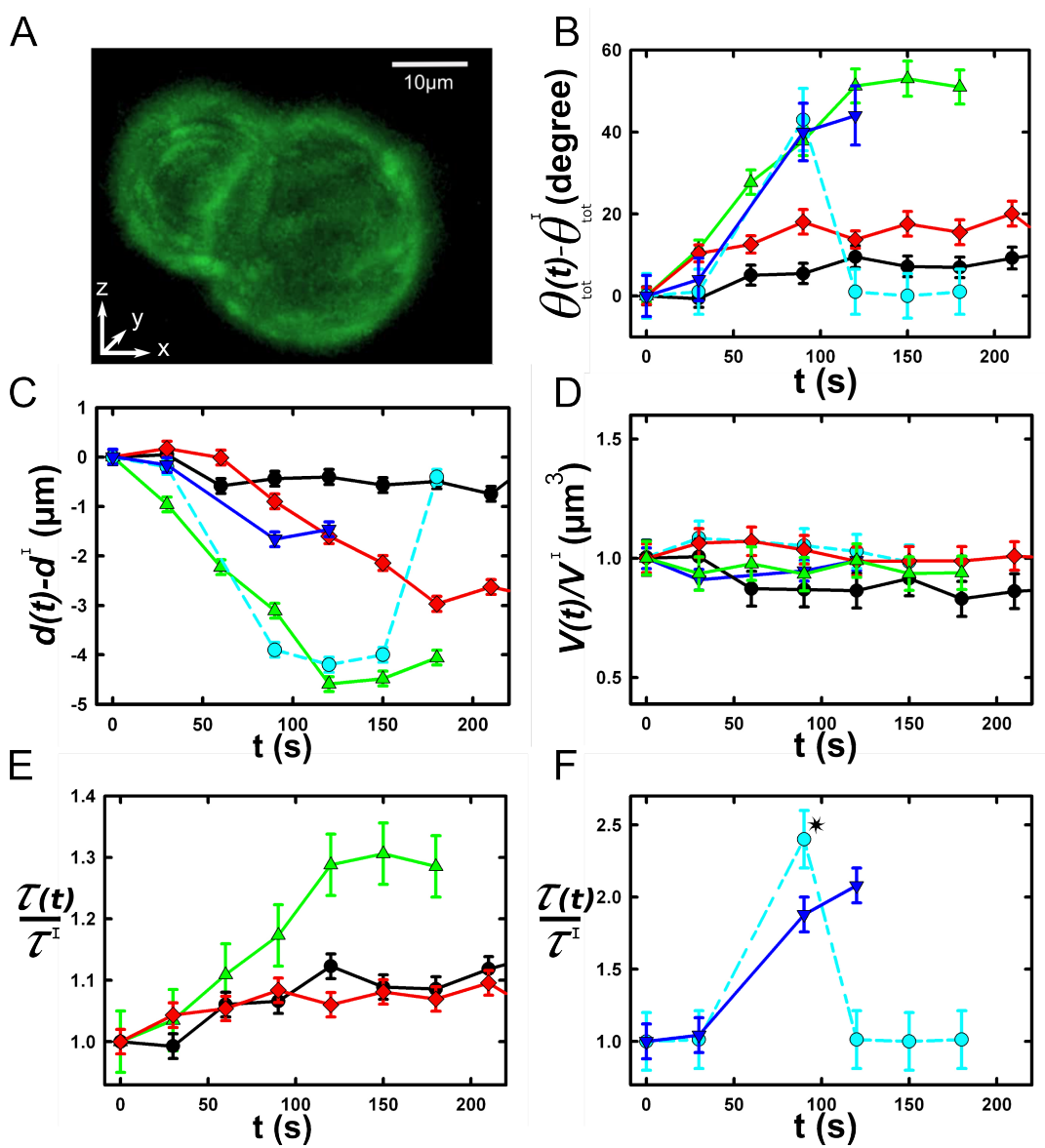
Figure 2: **Effect of an actin cortex on the doublet's shape.** A) Image of the same  
290 doublet coated with fluorescent actin before i) ii) and after iii) iv) actin cortex  
disruption. The actin cortex is visualized by epifluorescence ii) iv) and the doublet by  
292 phase contrast i) iii). Scale bar 5 $\mu$ m. B) Measurement of the contact angle between  
the two liposomes as a function of their volume, before (black) and after (white)  
294 disruption of the stabilized actin cortex. Error bars represent standard error.



296

298

Figure 3: **Geometrical parameters over time.** A) 3D reconstruction of a doublet surrounded by actin. Note that there is no actin on the membranes separating the two liposomes. Evolution of the contact angle (B), the distance between centers (C), compared with the initial ones as a function of time. Evolution of the volume ratio (D) and the tension ratio (E, F) compared with the initial ones as a function of time. Increase. B-F: each doublet is represented by a different colour and the blue dashed line corresponds to a doublet where cortex ruptures (\*).



306

308 **Methods.**

Lipids, reagents and proteins. Chemicals are purchased from Sigma Aldrich (St. Louis, MO, USA) unless specified otherwise. L-alpha-phosphatidylcholine (EPC) and 1,2-distearoyl-sn-glycero-3-phosphoethanolamine-N-[biotinyl polyethylene glycol 2000] (biotinylated lipids), 1,2-dioleoyl-sn-glycero-3-phosphocholine are purchased from Avanti polar lipids (Alabaster, USA). Actin and biotinylated actin are purchased from Cytoskeleton (Denver, USA) and used with no further purification. Fluorescent Alexa-488 actin is obtained from Molecular Probes. Monomeric actin containing 10% or 20% of labeled Alexa-488 actin and 0.25% of biotinylated actin is diluted in G-Buffer (2mM Tris, 0.2mM CaCl<sub>2</sub>, 0.2mM DTT at pH 8.0). Myosin II is purified from rabbit skeletal muscle and fluorescent myosin II is prepared as previously described [25] and its functionality is confirmed by motility assays showing an average gliding speed of  $4.5 \pm 1.5 \mu\text{m/s}$  ( $N = 27$ ) [26]. The working buffer contains 25 mM imidazole, 50 mM KCl, 70 mM sucrose, 1mM Tris, 2 mM MgCl<sub>2</sub>, 1 mM ATP, 0.1 mM DTT, 0.02 mg/ml  $\beta$ -casein, adjusted to pH 7.4. All proteins are mixed in the working buffer and myosin II forms minifilaments of approximately 0.7 micrometer length with about 100 motors [27].

**Formation of liposome doublets, actin cortices on doublets.** Liposomes are electroformed [18]. Briefly, 20  $\mu\text{L}$  of a mixture of EPC lipids and biotin PEG lipids present at 0.1 molar ratio with a concentration of 2.5 mg/ml in chloroform/methanol 5:3 (v:v) are spread on ITO-coated plates and dried under nitrogen flow, then placed under vacuum for 2 hours. A chamber is formed using the ITO plates (their conductive sides facing each other) filled with sucrose buffer (200mM sucrose, 2mM Tris adjusted at pH 7.4, containing or not sulforhodamin B 0.9  $\mu\text{M}$ ), and sealed with hematocrit paste (Vitrex medical, Denmark). Liposomes are formed by applying an

alternate current voltage (1V - 10 Hz) for 1hour and 15 minutes. Then liposomes are  
334 incubated with 160 nM streptavidin for 15 min and diluted 30 times. Note that for the  
observation of the interface between the doublet liposomes, we prepare separately  
336 liposomes in the presence or in the absence of sulforhodamin B, and mix them at  
equal volume before incubation with streptavidin. At this stage we have doublets  
338 coated with streptavidin. Waiting more than 15 min would increase the quantity of  
liposome aggregates and decrease the quantity of doublets and single liposomes. A  
340 bulk solution of 40  $\mu$ M actin monomers (Cytoskeleton, Denver USA) containing 10%  
fluorescently labeled actin and 1/400 biotinylated actin monomers is polymerized at 1  
342  $\mu$ M by diluting 40 times in the working buffer (25 mM imidazole, 50 mM KCl, 70 mM  
sucrose, 1mM Tris, 2 mM MgCl<sub>2</sub>, 1 mM ATP, 0.1 mM DTT, 0.02 mg/ml  $\beta$ -casein,  
344 adjusted at a pH 7.4) for 1 hour in the presence of 1  $\mu$ M of phalloidin (to prevent  
depolymerization). Actin filaments are then diluted 10-fold to 0.1  $\mu$ M, mixed with  
346 streptavidin-coated doublets of liposomes, and incubated for 15 min. The mix is  
diluted 5 times for observation to reduce background fluorescence from actin  
348 filaments.

**Observation chamber design, formation and myosin II injection.** Observation  
350 chambers are made by heating Parafilm stripes (as spacer) with an H-shape  
between two coverslips. The solution containing doublets is injected in the chamber  
352 and let few minutes in order to allow gentle sedimentation of the doublets (**Fig. 1C**).  
Then myosin II filaments are injected in the chamber and the H-shape and doublets  
354 are imaged over time in the middle of the chamber (**Fig. 1C**). Conditions  
(streptavidin, actin filament length) are the same as in [16] but observations are  
356 made before breakage of the acto-myosin shell.

**Observation of doublets.** Epifluorescence and phase contrast microscopy are  
358 performed using an IX70 Olympus inverted microscope with a 100x or a 60x oil-  
immersion objective. Spinning-disk confocal microscopy is performed on a Nikon  
360 Eclipse T1 microscope with an Andor Evolution Spinning Disc system and a 60x  
water immersion objective and a z distance between z-slices of 1/25 of the doublet  
362 size.

**Image processing and data analysis.** 2D-images: the contact angle is measured by  
364 adjusting two circles on binarised liposome images taken by phase contrast or  
epifluorescence microscopy. 3D-images: the geometrical parameters of the doublets  
366 are determined by optimizing the correlation between simulated and acquired 3D  
recording. Simulated 3D stacks, using [Python], [Numpy] and [Cython] are obtained  
368 by creating two spherical caps in contact and reproducing the fluorescent signal of  
actin at the external surface. Optimizing the correlation between simulated and  
370 acquired data is done using [Python] and [SciPy] (Nelder–Mead simplex method from  
the "optimize" submodule). Initial fit parameters of the first frame of each timelapse  
372 are determined visually. For the subsequent frame, we use the optimized parameters  
as initial parameters. Robustness of fit is checked by several repeats while changing  
374 the initial fit parameters by a random amount drawn from a normal distribution (mean  
0 $\mu$ m and standard deviation 0.5 $\mu$ m). The obtained eight parameters (2 centers with  
376 X,Y,Z coordinate and 2 liposomes radii) geometrically define the contact angle and  
the distance between centers. All the data processing was done in an [IPython]  
378 environment.